CASE REPORT

Nagoya J. Med. Sci. **85**. 844–851, 2023
doi:10.18999/nagjms.85.4.844

Ultra-high-density mapping for safe and effective typical atrioventricular nodal reentrant tachycardia ablation

Yusuke Sakamoto and Hiroyuki Osanai

Department of Cardiology, Tosei General Hospital, Nagoya, Japan

ABSTRACT

Ultra-high-density mapping was used for potential-guided radiofrequency ablation for typical atrioventricular nodal reentrant tachycardia. The mapping detailed the spread of activation in the Koch's triangle and identified target potentials and tachycardia circuits. This mapping provides additional information to the slow pathway conventionally used for safe and effective ablation.

Keywords: atrioventricular nodal reentrant tachycardia, Koch's triangle, rhythmia, slow pathway, ultra-high-density mapping

Abbreviations:
AVNRT: atrioventricular nodal reentrant tachycardia
CS: coronary sinus
FP: fast pathway
JP: Jackman potential
RF: radiofrequency
SP: slow pathway
SR: sinus rhythm
UHD: ultra-high-density

INTRODUCTION

Catheter ablation for typical atrioventricular nodal reentrant tachycardia (AVNRT) is an established effective treatment.[1] Conventional target sites for ablation include the slow potential of the slow pathway (SP)[2,3] or a specific anatomical site.[4] Recently, a detailed analysis of the excitatory propagation of the Koch's triangle in typical AVNRT was conducted using the Rhythmia electroanatomic mapping system,[5] with successful outcomes of ablation performed at the recording site of Jackman potentials (JPs), characterized by dull and spiky potentials on detailed mapping of the Koch's triangle using the same system.[6] Herein, we report our use of ultra-high-density (UHD) mapping to identify the ablation optimal site for the treatment of typical slow-fast AVNRT, diagnosed by electrophysiological study and established criteria.[7]

Received: November 24, 2022; accepted: January 18, 2023

Corresponding Author: Yusuke Sakamoto, MD, PhD
Department of Cardiology, Tosei General Hospital, 160 Nishi-Oiwake-cho, Seto 489-8642, Japan
Tel: +81-561-82-5101, Fax: +81-561-82-9139, E-mail: aimnaz_sheena@yahoo.co.jp

Written informed consent was obtained from all patients for the ablation procedure and enrollment in our study. This study was conducted following the approval of the hospital's Institutional Review Board. Ethics clearance was obtained from the Research Ethics Committee of the Tosei General Hospital. The study was conducted in accordance with the ethical standards laid down in the 1964 Declaration of Helsinki and its later amendments.

Briefly, our approach using UHD is as follows. Automated mapping of atrial activation during both sinus rhythm (SR) and tachycardia is performed using a basket catheter (64 electrodes; area, 0.4 mm^2; spacing, 2.5 mm; Orion, Boston Scientific, Natick, MA, USA) and the Rhythmia system (Rhythmia HDx SW, version 4.0, Boston Scientific). Bipolar electrograms are filtered (30–300 Hz), with unipolar electrograms set at a default value of 1–300 Hz. The coronary sinus (CS) electrogram is then used as a timing reference to map the SR and AVNRT. Ablation is performed using a 4-mm open-irrigated catheter (INTELLANAV STABLEPOINT, Boston Scientific), with a radiofrequency (RF) current (20–35 W; temperature-control mode, 45°C), delivered to a maximum of 30 s.

CASE REPORT

Case 1

The patient was a 50-year-old woman whose UHD map during SR is shown in Figure 1A. Annotations were automatically attached to the absolute peak, and automatic adjustments were conducted using the intelligent annotation function. When the His potential was visible, an annotation was readded to the His potential manually. Activation from the sinus node spreads to the fast pathway (FP) and then to the Koch's triangle. Subsequently, the activation was conducted to the SP, bypassing near the CS, and to the His bundle. Based on the local potentials recorded using the Orion system, the His potentials and JPs were marked to examine their distribution (His potentials are tagged in yellow and JPs in green; Figure 1B). The JPs, characterized by fragmented dull and spiky potentials, were distributed in the posterior septum, highlighted by the complex activation observed using the LUMIPOINT algorithm. During right ventricular pacing, antidromic conduction from the anterior septum was observed (Figure 1C). The site for RF ablation was selected based on an analysis of the spread of activation in the Koch's triangle and the distribution of local potentials. As this was our first case using UHD mapping to guide RF ablation and prioritizing patient safety, RF ablation was performed at a site closer to the ventricle than to the site JPs. This first site of ablation was ineffective and thus, we gradually moved the site of RF towards the atrial side. A junctional rhythm appeared with RF application at the site of the JP (red circle), with successful dissection of the SP achieved (Figure 1D). This site matched the highlighted site on the LUMIPOINT algorithm. A total of nine ablations were conducted.

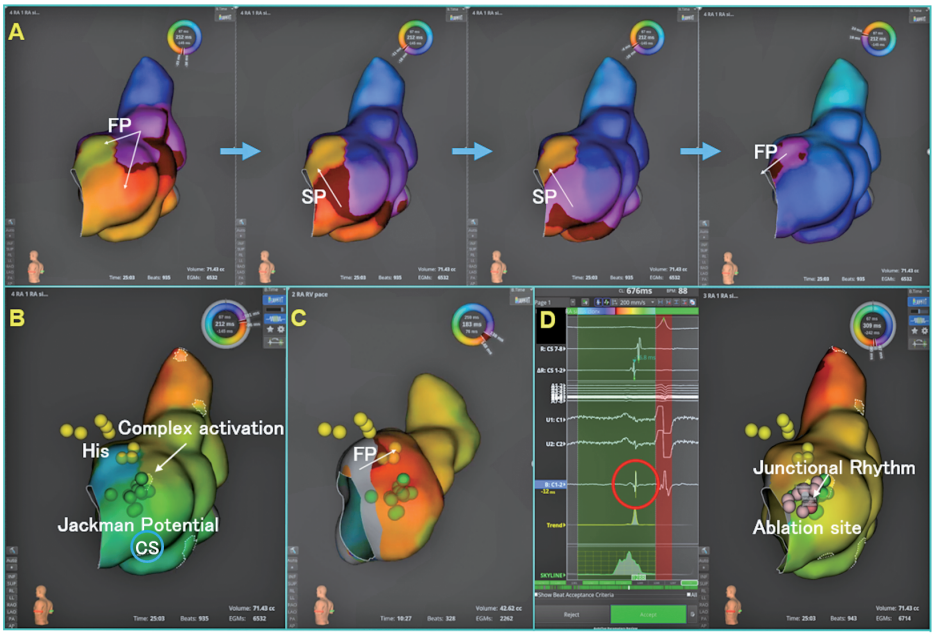

Fig. 1 Activation during sinus rhythm and slow pathway potentials in Case 1

Fig. 1A: Activation during SR, showing the spread of activation from the FP and the SP up to the His bundle.

Fig. 1B: Distribution of slow pathway potentials during SR. The JP is shown with a green tag and the His potential with a yellow tag. The JP is also shown on the LUMIPOINT algorithm.

Fig. 1C: Activation during RV pacing, showing ventriculoatrial conduction during RV pacing observed at the same site as the orthodromic conduction.

Fig. 1D: Ablation site and local potential observed with RF application at a recording site of the JP. A junctional rhythm appeared, with successful dissection of the SP achieved.

FP: fast pathway
SP: slow pathway
CS: coronary sinus
JP: Jackman potential
RF: radiofrequency
RV: right ventricle
SR: sinus rhythm

Case 2

The patient was a 65-year-old man whose UHD mapping and orthodromic conduction recording of the FP and SP during SR is shown in Figure 2A. Antidromic conduction from the anterior septum during right ventricular pacing was also observed (Figure 2B). Tachycardia was then induced and mapping during tachycardia was performed (Figure 2C). The V-overlap function was removed, and the point was obtained in an open window. The activation spread from the anterior septum to the atrium, matching the antidromic conduction observed during right ventricular pacing, then proceeding around a functional block line, with orthodromic conduction of the SP, as observed during the SR. In this case, JPs were observed at the site of SP conduction in the posterior septum. A junctional rhythm appeared with RF application at this site, with successful dissection of the SP achieved with a total of four ablations. Therefore, in this case, as a useful aid for ablation using JPs during sinus rhythm as an index, the optimal site for ablation was accurately identified as the tachycardia circuit determined by mapping during tachycardia.

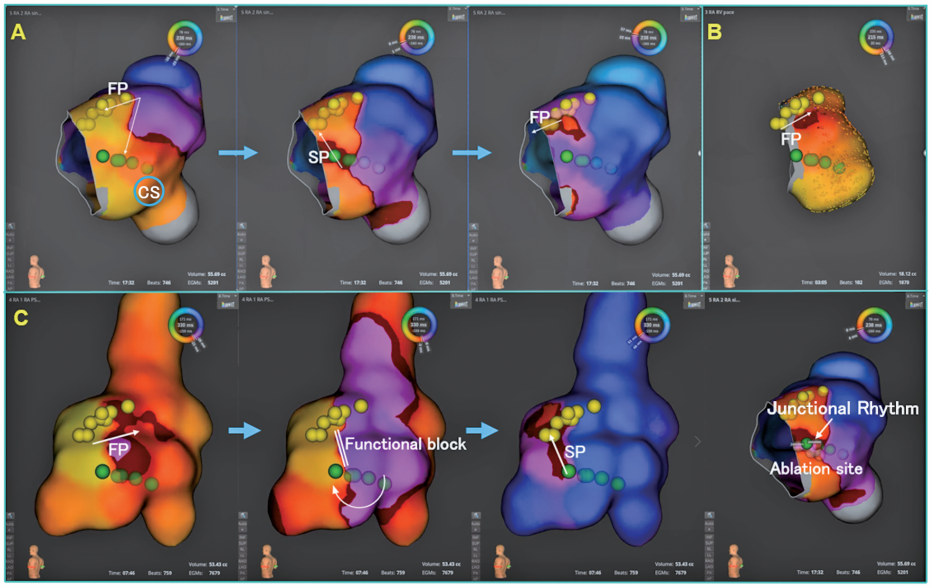

Fig. 2 Tachycardia mapping in Case 2

Fig. 2A, 2B: Activation during SR (A) and RV (B) pacing. Ventriculoatrial conduction during RV pacing is observed at the same site as the orthodromic conduction.

Fig. 2C: Tachycardia mapping, showing that the tachycardia circuit matched the orthodromic conduction and antidromic conduction visualized during SR and RV pacing. Identification of the optimal site for ablation allowed successful dissection of the SP to be achieved.

FP: fast pathway
CS: coronary sinus
SP: slow pathway
RV: right ventricle
SR: sinus rhythm

Case 3

The patient was a 57-year-old woman whose UHD mapping is shown in Figure 3A. Mapping included activation spread during SR, with a strongly evident SP observed. On subsequent burst pacing of the CS ostium, orthodromic conduction of the SP was observed, allowing mapping of SP conduction (Figure 3B). No FP conduction was observed during the refractory period, which allowed observation of the SP alone. This matched the SP conduction observed during SR. RF ablation was performed at the site of the JPs, with a junctional rhythm observed. A total of seven ablations were conducted. The JP site matched the SP visualized during CS pacing (Figure 3C).

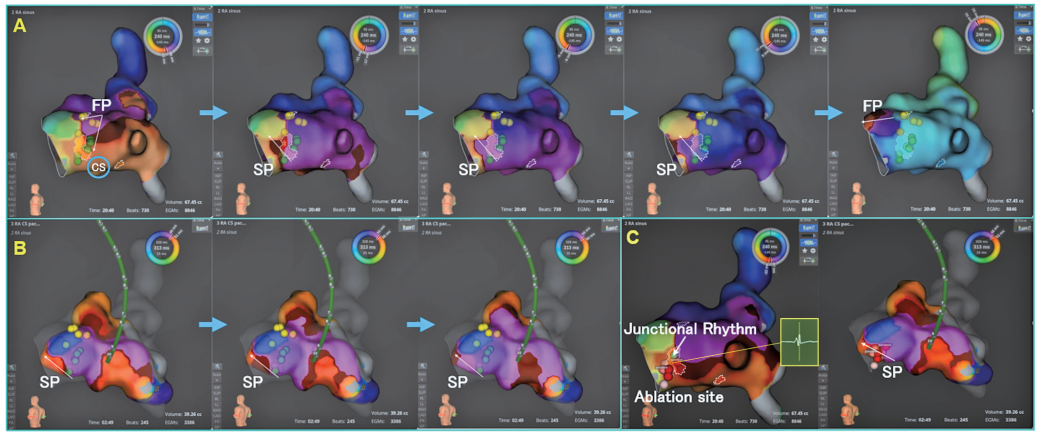

Fig. 3 Analysis of the activation spread of the slow pathway for Case 3
Fig. 3A: Activation during SR, with the JP observed in the posterior septum; this site was also highlighted by the LUMIPOINT algorithm. SP conduction is also visualized at this site.
Fig. 3B: Activation during CS ostium pacing, with only the SP conduction visualized. The conduction matched the conduction visualized during SR.
Fig. 3C: Ablation site matched the SP site visualized during CS ostium pacing.
FP: fast pathway
SR: sinus rhythm
JP: Jackman potential
SP: slow pathway
CS: coronary sinus

Case 4

The patient was an 81-year-old man, in whom JPs were not observed, with no fragmented potentials observed in the Koch's triangle (Figure 4A) and no highlighted area on the LUMIPOINT algorithm (red circle). RF was first applied to the posterior septum, which was ineffective. The

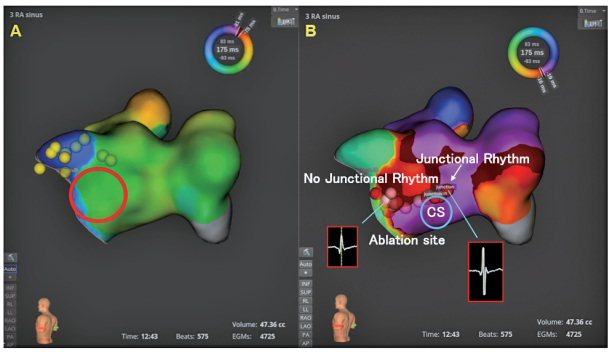

Fig. 4 The absence of slow pathway potentials in Case 4
Fig. 4A: Search for potentials during SR with no JP visualized after careful search using the Orion system.
Fig. 4B: Ablation site located inside the roof of the CS.
SR: sinus rhythm
JP: Jackman potential
CS: coronary sinus

site of RF was then gradually moved to the upper site, which was also ineffective. A junctional rhythm appeared with RF application to the roof of the CS, with successful dissection of the SP achieved (Figure 4B). No fragmented potentials were observed at the first site of RF application or the successful ablation site.

DISCUSSION

Previous studies have reported an association between the rightward and leftward inferior extensions of the compact AV node, the SP, and JPs.[8] The characteristics of the local potentials in Case 1 are shown in Figure 5A. The conduction from the FP (blue line) shows a normal potential in the atrium. At the sites of recording of JPs (green lines), the height of the spiky potential was greater at sites closer to the His bundle and where His potentials were recorded (yellow lines). The presence of spiky potentials may, therefore, indicate the local potentials in the rightward inferior extension of the AV node, while the fragmented potentials observed at the site of recording of JPs may be indicative of the presence of transitional tissue.

In the absence of spiky potentials, even in the presence of fragmented potentials, a junctional rhythm was not observed with RF application when SP was unsuccessful (Figure 5B). Based on this finding, spiky potentials might reflect potentials of the right inferior extension of the AV node. Therefore, unless RF heat reaches spiky potentials, dissection of the SP will likely be unsuccessful. The LUMIPOINT algorithm is useful as an aid in determining the ablation site; however, given their importance, JPs need to be duly confirmed.

The isochronal late activation map in Case 1 (Figure 5C) shows that conduction at a site close to the FP and the bundle of His is fast, with a delay in the conduction from transitional tissue in the right inferior extension. This delay is reflected in the recorded JPs, with ablation at this site being successful.

The findings in Case 2 confirm the importance of UHD mapping to visualize the tachycardia circuit and, thus, identifying the optimal site for safe and effective RF ablation. The UHD mapping would be particularly useful when an RF site is difficult to determine using a perspective image alone, such as in the presence of anatomical rotation. Of note, tachycardia mapping was performed within 7 min in Case 2, which did not significantly increase the duration of the procedure.

In Case 3, it was possible to visualize the SP conduction alone. The highlighted site on the LUMIPOINT algorithm and the site of successful RF ablation matched the visualized SP conduction on UHD. Visualization of the course of SP conduction alone up to the His bundle is an effective method of depicting the route of SP alone, which was not clear on 3D mapping, until now.

In Case 4, JPs were not observed and the site of successful ablation was on the CS roof. Of the 10 cases of RF ablation guided by UHD, the absence of JPs was only observed in Case 4; in all other cases, a junctional rhythm appeared at a site with the JP and dissection of the SP was successful. A previous study reported that dissection of the SP was not successful in approximately 5% of cases of slow/fast AVNRT, despite ablation being performed at a site at which the JP was recorded. It was suggested that in these patients, the leftward inferior extension of the AV node may form the antegrade SP in the entrant circuit.[8] In Case 4, successful dissection of the SP was achieved on the roof of the CS ostium, indicative of the possibility that the leftward inferior extension formed the antegrade SP.

In summary, UHD mapping provided a high-resolution three-dimensional map of local potentials and tachycardia circuits to identify safe and effective RF ablation sites for AVNRT. The complementary use of the LUMIPOINT allowed for analysis of fragmented potentials. Using

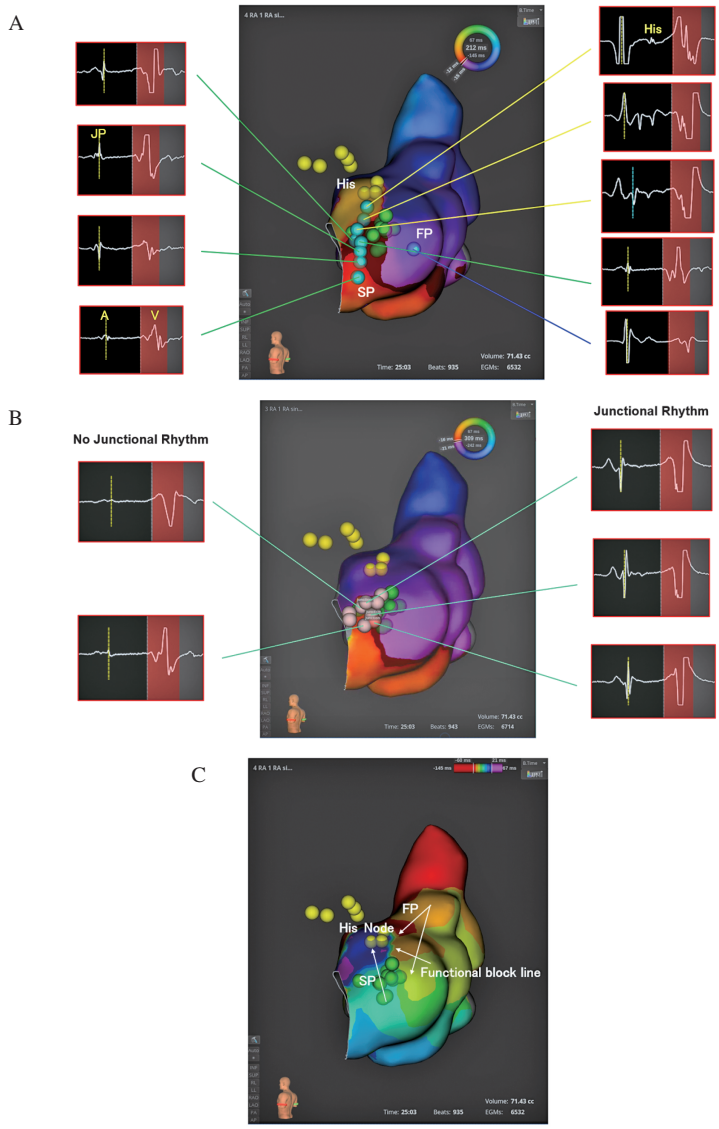

Fig. 5 Characteristics and analysis of local potentials in Case 1

Fig. 5A: Characteristics of local potentials, showing the spread of activation from the FP (blue line), the JP (green lines), and the His potential (yellow lines). The height of the spiky JP increased as the site was in a higher position and the potentials split into the His potentials.

Fig. 5B: Visualization of local potentials and junctional rhythm. The junctional rhythm appeared with ablation at the recording site of spiky potentials, with successful dissection of the SP achieved.

Fig. 5C: Isochronal late activation map showing the speed of activation spread and slow conduction of the SP. At the site where activation entered the SP, the path of conduction turned in the vicinity of the CS and a functional block line was observed.

FP: fast pathway
SP: slow pathway
A: atrium
V: ventricle
JP: Jackman potential
CS: coronary sinus

this method, in our case series, there was no incidence of ablation-induced atrioventricular blocks and the SP was successfully transected in all cases.

AUTHOR CONTRIBUTIONS

Yusuke Sakamoto: Conceptualization; Data curation; Formal analysis; Investigation; Methodology; Project administration; Software; Supervision; Validation; Visualization; Roles/Writing – original draft; Writing – review & editing.

Hiroyuki Osanai: Project administration.

ACKNOWLEDGEMENTS

We acknowledge and appreciate the co-medical staff working on our ablation team.

CONFLICTS OF INTEREST AND FUNDING

The authors have no conflicts of interests related to this study to declare. This research did not receive any specific grant from funding agencies in the public, commercial, or not-for-profit sectors.

REFERENCES

1 Katritsis DG, Zografos T, Katritsis GD, et al. Catheter ablation vs. antiarrhythmic drug therapy in patients with symptomatic atrioventricular nodal re-entrant tachycardia: a randomized, controlled trial. *Europace.* 2017;19(4):602–606. doi:10.1093/europace/euw064.

2 Jackman WM, Beckman KJ, McClelland JH, et al. Treatment of supraventricular tachycardia due to atrioventricular nodal reentry by radiofrequency catheter ablation of slow-pathway conduction. *N Engl J Med.* 1992;327(5):313–318. doi:10.1056/NEJM199207303270504.

3 Haissaguerre M, Gaita F, Fischer B, et al. Elimination of atrioventricular nodal reentrant tachycardia using discrete slow potentials to guide application of radiofrequency energy. *Circulation.* 1992;85(6):2162–2175. doi:10.1161/01.cir.85.6.2162.

4 Nogami A, Kurita T, Abe H, et al. CORRIGENDUM: JCS/JHRS 2019 guideline on non-pharmacotherapy of cardiac arrhythmias. *Circ J.* 2021;85(9):1692–1700. doi:10.1253/circj.CJ-66-0196.

5 Chua K, Upadhyay GA, Lee E, et al. High-resolution mapping of the triangle of Koch: Spatial heterogeneity of fast pathway atrionodal connections. *Heart Rhythm.* 2018;15(3):421–429. doi:10.1016/j.hrthm.2017.10.030.

6 Pandozi C, Lavalle C, Bongiorni MG, et al. High-density mapping of Koch's triangle during sinus rhythm and typical AV nodal reentrant tachycardia: new insight. *J Interv Card Electrophysiol.* 2021;61(3):487–497. doi:10.1007/s10840-020-00841-8.

7 Knight BP, Ebinger M, Oral H, et al. Diagnostic value of tachycardia features and pacing maneuvers during paroxysmal supraventricular tachycardia. *J Am Coll Cardiol.* 2000;36(2):574–582. doi:10.1016/s0735-1097(00)00770-1.

8 Nakagawa H, Jackman WM. Catheter ablation of paroxysmal supraventricular tachycardia. *Circulation.* 2007;116(21):2465–2478. doi:10.1161/CIRCULATIONAHA.106.655746.